Tetratricopeptide repeat protein protects photosystem I from oxidative disruption during assembly

Mark Heinnickel[a,1], Rick G. Kim[a,b,1,2], Tyler M. Wittkopp[a,b], Wenqiang Yang[a], Karim A. Walters[c], Stephen K. Herbert[a,d], and Arthur R. Grossman[a]

[a]Department of Plant Biology, Carnegie Institution for Science, Stanford, CA 94305; [b]Department of Biology, Stanford University, Stanford, CA 94305; [c]Department of Chemistry, Pennsylvania State University, University Park, PA 16802; and [d]Department of Plant Sciences, University of Wyoming, Laramie, WY 82071

Edited by Bob B. Buchanan, University of California, Berkeley, CA, and approved January 28, 2016 (received for review December 8, 2015)

A *Chlamydomonas reinhardtii* mutant lacking CGL71, a thylakoid membrane protein previously shown to be involved in photosystem I (PSI) accumulation, exhibited photosensitivity and highly reduced abundance of PSI under photoheterotrophic conditions. Remarkably, the PSI content of this mutant declined to nearly undetectable levels under dark, oxic conditions, demonstrating that reduced PSI accumulation in the mutant is not strictly the result of photodamage. Furthermore, PSI returns to nearly wild-type levels when the O_2 concentration in the medium is lowered. Overall, our results suggest that the accumulation of PSI in the mutant correlates with the redox state of the stroma rather than photodamage and that CGL71 functions under atmospheric O_2 conditions to allow stable assembly of PSI. These findings may reflect the history of the Earth's atmosphere as it transitioned from anoxic to highly oxic (1–2 billion years ago), a change that required organisms to evolve mechanisms to assist in the assembly and stability of proteins or complexes with O_2-sensitive cofactors.

oxidative disruption | photosystem I biogenesis | photosynthesis | GreenCut

Although the structure and function of photosystem I (PSI) in plants, algae, and cyanobacteria have been elucidated at high spatial and temporal resolution (1–7), PSI assembly is poorly understood but is a topic of growing interest (7). Unlike PSII, there are essentially no inhibitors of PSI, and PSI assembly intermediates are difficult to separate from mature complexes (7–9). Furthermore, PSI abundance is not highly controlled by environmental conditions (8), and mutants with much lower levels of PSI than WT cells can still grow under photoautotrophic conditions (10, 11), although they often are light sensitive (12, 13) and the level of PSI in a mutant may not show a linear correlation with its rate of photoautotrophic growth.

Progress in understanding PSI assembly has come largely from studies of mutants in putative assembly factors (7, 10, 11, 14, 15), including hypothetical chloroplast open reading frame 3 (Ycf3), Ycf3-interacting protein 1 (Y3IP1), Ycf4, plant-specific putative DNA-binding protein 1 (PPD1), and Ycf37/pale yellow green7-1 (Pyg7-1). Ycf3 is a plastid-encoded protein with tetratricopeptide repeat (TPR) domains believed to interact transiently with PsaA and PSAD (16), whereas Y3IP1 interacts with Ycf3 (10). Ycf4 has two transmembrane domains and is necessary for PSI assembly in Chlamydomonas, but tobacco mutants lacking Ycf4 accumulate sufficient PSI to grow photoautotrophically (11). ALB3 (ALBINO3) mediates the insertion of the chloroplast-encoded core PSI proteins, PsaA and PsaB, into thylakoid membranes (17) but also is involved in the biogenesis of other photosynthetic complexes (7, 18, 19). PPD1 is required for establishing proper structure/function relationships for the luminal portion of PSI (15).

One of the least understood of the proteins associated with PSI assembly is the Chlamydomonas protein CGL71. This protein is part of the GreenCut, a bioinformatically assembled set of proteins present in all green lineage organisms examined; many of these proteins are associated with photosynthetic function (20–25). CGL71 is orthologous to Ycf37 of *Synechocystis* (26) and PYG7 of *Arabidopsis* (27). In this study, we present evidence that supports a role for CGL71 in PSI assembly and, more specifically, in protecting the complex from oxidative disruption during assembly. The requirement of CGL71 for proper assembly of PSI may reflect an evolutionary adaptation that is linked to oxygenation of the Earth's atmosphere.

Results

The *cgl71* Mutant Is Impaired in Photosynthesis. CGL71 is a TPR protein integral to thylakoid membranes. A Chlamydomonas *cgl71* mutant was identified with the insertion of the *ble* (bleomycin/zeocin resistance) marker gene in the first exon of the *CGL71* gene (Fig. S1*A*). This mutation caused a loss of gene function: The mutant synthesized a highly truncated protein with the C-terminal 43 amino acids differing from the sequence of the WT protein, as shown in Fig. S1*C*. Unlike WT cells, the mutant exhibited no photoautotrophic growth in the light on minimal agar high-salt (HS) medium (Fig. S1*B*), indicating its inability to perform normal photosynthesis. Growth on solid medium was similar for mutant and WT cells in the presence of a fixed carbon source (Tris-acetate phosphate medium, TAP) either in the dark (heterotrophically) or in low-intensity light (mixotrophically), but the mutant grew slowly or not at all at higher light intensities (50 μmol photons·m^{-2}·s^{-1} and higher), whereas these higher intensities supported vigorous growth of WT cells and the rescued strain (Fig. 1*A*).

The rates of photosynthetic O_2 evolution at various light intensities (Fig. 1*B*) were somewhat lower in the *cgl71* mutant than in WT cells

Significance

Our results demonstrate that *Chlamydomonas reinhardtii* CGL71, a tetratricopeptide repeat protein, is involved in protecting photosystem I from oxidative disruption during assembly; this process may reflect oxygen sensitivity of the iron sulfur clusters that are integral to the complex. During the early evolution of photosynthesis, the atmosphere of the Earth was anoxic, making protection of complexes and assembly processes from the highly reactive oxygen molecule unnecessary. However, as atmospheric oxygen accumulated, mechanisms and factors evolved to stabilize the complexes during assembly. This need for oxidative protection is not exclusive to the photosynthetic machinery but would apply to any complex with cofactors and features susceptible to oxidizing conditions.

Author contributions: M.H., R.G.K., T.M.W., W.Y., K.A.W., S.K.H., and A.R.G. designed research; M.H., R.G.K., T.M.W., W.Y., K.A.W., and S.K.H. performed research; W.Y. and K.A.W. contributed new reagents/analytic tools; M.H., R.G.K., T.M.W., W.Y., K.A.W., S.K.H., and A.R.G. analyzed data; and M.H., R.G.K., T.M.W., S.K.H., and A.R.G. wrote the paper.

The authors declare no conflict of interest.

This article is a PNAS Direct Submission.

[1]M.H. and R.G.K. contributed equally to this work.

[2]To whom correspondence should be addressed. Email: rgkim9@gmail.com.

This article contains supporting information online at www.pnas.org/lookup/suppl/doi:10.1073/pnas.1524040113/-/DCSupplemental.

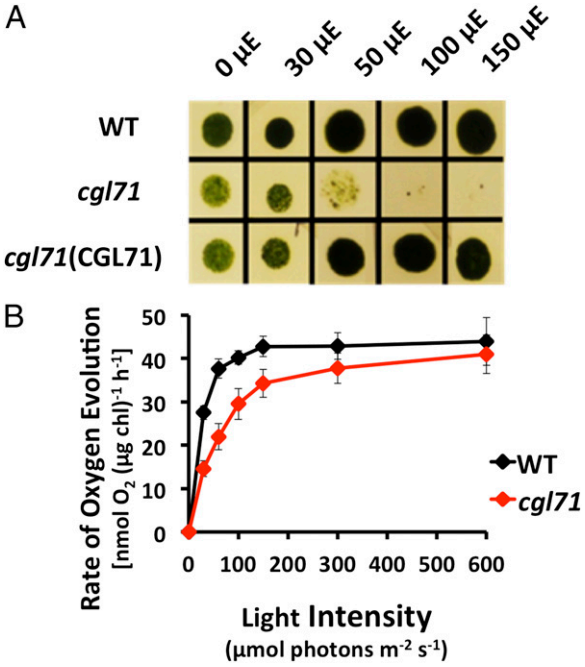

Fig. 1. Growth and O_2 evolution of the *cgl71* mutant. (*A*) WT, *cgl71*, and *cgl71* (CGL71) rescued cells were grown at 30 µmol photons·m^{-2}·s^{-1} (µE) in liquid TAP medium and then were washed and spotted onto solid TAP medium and allowed to grow for 5 d at various light intensities, as indicated at the top of the image. (*B*) Rate of O_2 evolution of WT and *cgl71* mutant cells after growth at 30 µE. Cells were pelleted by centrifugation (3,200 × *g*) for 10 min, resuspended in 50 mM Hepes (pH 7.5) containing 5 mM $NaHCO_3$, and shaken in the dark for 30 min. During the assay, samples were illuminated at increasing light intensities, as indicated on the *x* axis, for 2 min each, followed by a 2-min dark incubation. The rate of O_2 evolution at each light intensity was corrected for the rate of dark respiration. Each point represents the mean of three biological replicates.

after growth in TAP medium at 30 µmol photons·m^{-2}·s^{-1} with moderate shaking (150 rpm), the conditions designated as low-light oxic (LO) conditions. At saturating light intensities, the rate of O_2 evolution in the *cgl71* mutant was about 77% of that in WT cells on a per-cell basis but was only ∼5% lower when the samples contained the same chlorophyll (chl) amount (Fig. 1*B*). At the lowest light intensities used, O_2 evolution was reduced by roughly 50% in the *cgl71* mutant.

Photosynthetic Electron Transport Is Altered in *cgl71*. ΦPSII, a chl fluorescence parameter that indicates the proportion of light being absorbed by PSII-associated antenna complexes and used by PSII for photochemistry (28, 29), was measured for WT cells, the *cgl71* mutant, and the complemented strain at different light intensities (Fig. 2*A*). Cells were grown in liquid TAP medium under LO conditions before ΦPSII measurements. Despite the small reduction of O_2 evolution per chl (µg) at saturating light intensities (Fig. 1*B*), *cgl71* exhibited a striking reduction of ΦPSII relative to WT cells at all but the lowest light intensities used. This result implies that the plastoquinone pool was much more reduced in the mutant than in the WT cells.

Rescue of Mutant Phenotype with *CGL71*. Based on results with 16 tetrads (Fig. S2), it was determined that the acetate-requiring and light-sensitive *cgl71* phenotypes cosegregated with the *ble* insertion. These results suggested that the *cgl71* phenotype was a consequence of this insertion, and this notion was confirmed by introducing a WT copy of *CGL71* into the *cgl71* mutant. Ectopic expression of the *CGL71* gene in mutant cells rescued both the growth phenotypes (Fig. 1*A* and Fig. S1*B*) and the defect in photosynthetic electron transport (PET) (Fig. 2*A*).

PSI Abundance Is Reduced in *cgl71* Cells. To identify the cause(s) of restricted PET and O_2 evolution in *cgl71*, we characterized photosynthetic activities of *cgl71*, WT, and the *cgl71*(CGL71) rescued strain. Table 1 shows functional measurements of various photosynthetic parameters from cells grown in liquid TAP medium under LO conditions. The results were consistent with an ∼70% decrease in PSI abundance (Table 1); there was little change in the level of PSII function as assayed by the maximum quantum yield (F_v/F_m) values (Fig. 2*A* and Table 1, ΦPSII after incubation at 0 light) or in the quantity of active cytochrome b_6f complex (cyt b_6f) (Table 1 and Fig. S3). Immunoblot analysis of polypeptides of the photosynthetic apparatus, shown in Fig. 2*B*, confirmed that the mutant is deficient for PSI polypeptides (PsaA, PsaC, PSAD, and PSAH) relative to both WT cells and the complemented strain (normalized to tubulin abundance) after growth under LO conditions. Levels of polypeptide subunits of other photosynthetic complexes, including the ATP synthase (AtpB), cyt b_6f (PetA), PSII (PsbB), Rubisco (RbcL), light-harvesting complexes (LHCA1, LHCB2), and PSI assembly factors (Ycf3 and Ycf4) were very similar in mutant and WT cells.

Electron Flow per PSI Is More Rapid in *cgl71* Cells than in WT Cells. Although the decrease in PSI content of *cgl71* cells was ∼70%, the decrease in light-saturated O_2 evolution was only 5% on a per-chl basis. One explanation for this result is that linear electron flow (LEF) per PSI is more rapid in *cgl71* than in WT cells; PSI is not the rate-limiting step of LEF, and the ratios of plastocyanin [PC; electron donor to photosystem I primary donor (P700)] and cyt *f* (the rate-limiting factor for LEF) to P700 are high in *cgl*71 cells (see Fig. 2*B* for PC and Table 1 and Fig. S3 for cyt *f*). To examine the kinetics of delivery of electrons to PSI based on examination of cyclic electron flow (CEF), WT and *cgl71* cells were incubated with the PSII inhibitors 3-(3,4-dichlorophenyl)-1-1-dimethylurea (DCMU) and hydroxylamine (HA) (these chemicals allow quantification of total $P700^+$ and the rate of its rereduction by CEF). As shown in Fig. 3*A*, irradiation with 156 µmol photons·m^{-2}·s^{-1} in the presence of DCMU and HA caused significant oxidation of P700 in WT cells as judged by bleaching at 705 nm, with full oxidation achieved by a saturating pulse (arrow in Fig. 3*A*). Under similar conditions, the *cgl71* mutant exhibited some P700 oxidation when the cells were exposed to 156 µmol photons·m^{-2}·s^{-1}, and the oxidation increased to the maximum with a saturating pulse. The total amount of oxidized $P700^+$ was ∼36% of that observed for WT cells (normalized to chl; Fig. 3*A*). After the saturating pulse, *cgl71* cells exhibited more rapid rereduction of $P700^+$ than WT cells (Fig. 3*B*), indicating that the CEF through PSI was more rapid in *cgl71* than in the WT cells. In the absence of DCMU, rereduction of cyt *f* was similar in the WT and mutant strains following the oxidizing flash (Fig. S3), indicating that all electron flow (both CEF and LEF) occurs at the same rate in WT and the *cgl71* mutant, even though the mutant has a reduced level of PSI.

To determine if total electron flow through PSI was more rapid in *cgl71* than in WT cells, we examined methyl viologen (MV)-catalyzed O_2 consumption by thylakoid membranes in a broken cell preparation. As shown in Fig. S4, oxygen consumption (normalized to chl) was similar for WT cells and the *cgl71* mutant at both moderate and very high light intensities, suggesting that electron flow through PSI is much more rapid in *cgl71* cells than in WT cells (because there are many fewer PSI reaction centers in *cgl71* cells than in WT cells on a per-chl basis). Furthermore, to confirm that the rapid rereduction of $P700^+$ in *cgl71* was not caused by recombination in damaged complexes, charge recombination was measured in purified thylakoid membranes in WT cells and in the *cgl71* mutant. As shown in Fig. S5, the kinetics of $P700^+$ charge recombination display a monoexponential decay with a $t_{1/2}$

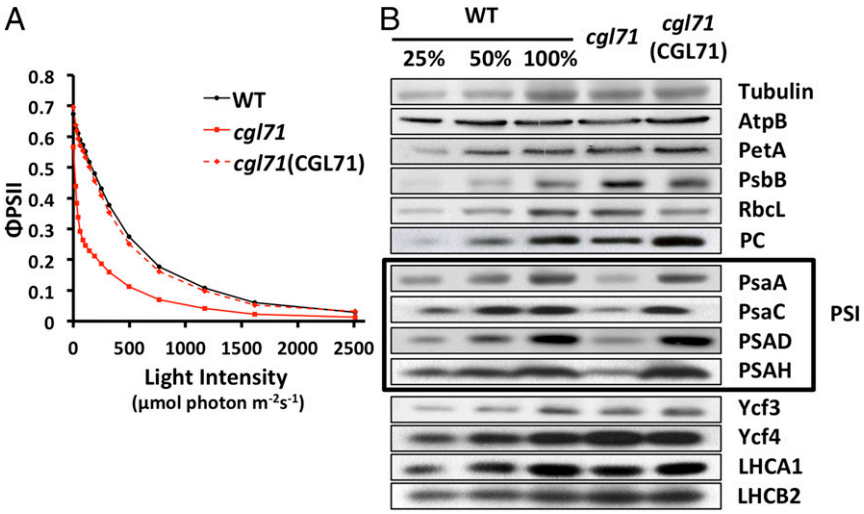

Fig. 2. Decreased PSII quantum yield and reduced levels of PSI polypeptides in the *cgl71* mutant. (*A*) Quantum yield of PSII based on the fluorescence parameter ΦPSII, which is $(F_m' - F_s)/F_m'$, in WT, *cgl71*, and the *cgl71*(CGL71) rescued strains. Cells used for the analyses were in exponential growth phase under LO conditions. For measurements, samples were exposed to 1 min of actinic light at the intensities indicated on the *x* axis. All values on the *y* axis are averages of three separate measurements (biological replicates). (*B*) Chlamydomonas proteins from WT, *cgl71*, and the *cgl71*(CGL71) rescued strain were resolved by SDS/PAGE on a 15% polyacrylamide gel and detected immunologically. Antibodies used for the analysis were to the polypeptides indicated at the right side of the figure. One microgram of chl was loaded for each sample analyzed. The boxed area highlights the subunit polypeptides of PSI. See *Materials and Methods* for more details. AtpB, β subunit of ATP synthase; LHCA1, light-harvesting polypeptides of PSI; LHCB2, light-harvesting polypeptide of PSII; PetA, cytochrome *f*; PsaA, PsaC, PSAD, and PSAH, polypeptide subunits of PSI; PsbB, chlorophyll protein of PSII; RbcL, large subunit of ribulose 1,5 bisphosphate carboxylase; Ycf3 and Ycf4, assembly factors associated with PSI.

of ∼36 ms. This result indicates that the terminal PSI electron acceptor is F_A/F_B in both WT cells and the *cgl71* mutant (30). Despite this higher overall rate of electron flow per PSI, O_2 evolution is slightly lower per cell (because there are many fewer PSI complexes per cell), implying that the relationship between PSI levels and the rate of light-saturated, whole-chain electron transport is not linear.

Reduced PSI Accumulation in *cgl71* Cells Is a Consequence of the Oxidative Environment. To determine if the lower level of PSI in *cgl71* was a consequence of photodamage, the mutant was grown heterotrophically in the dark. Surprisingly, maintaining the cells in complete darkness in TAP medium with shaking at 150 rpm in air [designated dark oxic (DO) conditions] had exactly the opposite effect on PSI activity/accumulation than would be expected if light were sensitizing PSI to photodamage. As shown in Fig. 4*A*, the $P700^+$/chl ratio decreased by ∼94% in *cgl71* following 3 d of growth in the dark. This finding was reflected in the immunoblot analysis shown in Fig. 4*B*, which demonstrated that the PsaC and PSAD subunits declined to undetectable levels and the PsaA subunit decreased by ∼95%.

Based on studies of ATP synthase activity, the redox state of the chloroplast stroma is likely to be more oxidizing in darkness than under illumination (31, 32). To determine if this presumed, more positive redox state impacts PSI biogenesis, the *cgl71* mutant was grown in the dark in TAP medium and exposed to an atmosphere of 10% air balanced with 90% N_2 at a flow rate of 400 mL/min with stirring at 600 rpm [designated the dark hypoxic (DH) condition] to generate a more reducing cellular environment. As shown in Fig. 4*A*, hypoxia caused the PSI level in *cgl71* to increase to ∼70% of the level of WT cells grown under the same conditions. This increase in active PSI under DH conditions also was reflected by increased accumulation of PSI polypeptide subunits, as observed by immunoblot analyses (Fig. 4*B*). To determine if the PSI that accumulated in the mutant under hypoxic conditions was active, DH-grown cells were analyzed for $P700^+$ rereduction kinetics. As shown in Fig. 3*B*, $P700^+$ rereduction by CEF in DH-grown *cgl71* cells became slower, approaching the kinetics observed in DH-grown WT cells. These results indicated that the mutant phenotype is strongly impacted by internal redox/oxic conditions: Under LO conditions, the assembly or stability of the PSI reaction centers is compromised, whereas the centers appear to accumulate to nearly WT levels under DH conditions.

Discussion

Studies of the function of CGL71 orthologs have been limited. The *ycf37* mutant of *Synechocystis* was shown to be deficient in PSI stability or biosynthesis (26), although the lesion only caused an ∼25% reduction in PSI accumulation with no observable change in growth or PET. The *pyg7* mutant of *Arabidopsis* exhibited a severe phenotype, with a complete loss of PSI and no photoautotrophic growth (27). The *cgl71* mutant in Chlamydomonas displays a phenotype intermediate between that of Δ*ycf37* of *Synechocystis* and *pyg7* of *Arabidopsis*. Similar to Δ*ycf37*, *cgl71* accumulated

Table 1. Summary of photosynthetic parameters: Maximum efficiency of PSII (F_v/F_m), chl *a*:*b* ratios, cyt b_6f/chl, P700/chl, and the ratio of PSI to PSII

Strain	F_v/F_m	chl *a*:*b*	cyt *f*/chl*	P700/chl*	PSI/PSII
WT	0.68 ± 0.01	1.94 ± 0.02	1.07 ± 0.34	3.32 ± 0.29	1.03 ± 0.04
cgl71	0.65 ± 0.01	1.84 ± 0.02	1.38 ± 0.10	1.02 ± 0.41	0.43 ± 0.02
cgl71(CGL71)	0.62 ± 0.01	1.96 ± 0.05	1.19 ± 0.33	3.19 ± 0.12	0.92 ± 0.04

Samples were collected during exponential growth in TAP medium under LO conditions. Values are means ± SD.
*Expressed in nanomoles per milligram total chl; values are an average of 10 replicates.

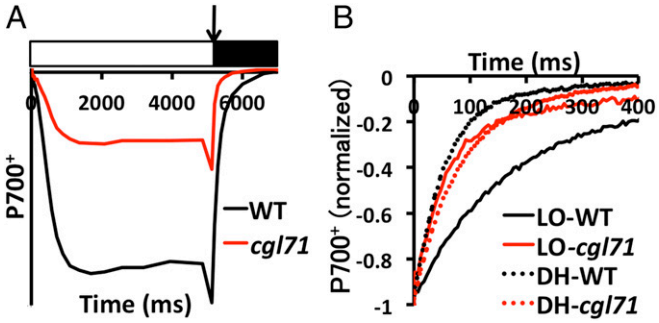

Fig. 3. The *cgl71* mutant is defective for active P700. (*A*) Oxidation and reduction characteristics of the *cgl71* mutant. Cells used for analyses were grown under LO conditions. Absorbance differences were monitored at 705 nm during continuous illumination of cells with 156 μmol photons·m^{-2}·s^{-1} for 5 s (white box), followed by a saturating light pulse (arrow) and a 2-s dark incubation (black box). WT and *cgl71* samples were concentrated to 30 μg chl/mL. Values on the *y* axis decrease as a greater amount of P700 is oxidized. The PSII inhibitors DCMU and HA were included at concentrations of 10 μM and 1 mM, respectively, to block all electron flow from PSII. (*B*) Kinetics of $P700^+$ rereduction following a saturating pulse as in *A* and normalized to total oxidizable P700. For all experiments, values on the *y* axis are the average of six measurements (technical replicates), which were essentially identical for all biological replicates. Error bars are not shown, but each data point shown in the figure does not deviate from any of the individual replicates (at least three for each data point) by more than 5% of the indicated value.

PSI, but the level was ∼70% less than that of WT cells under LO conditions in the presence of acetate. Similar to the *pyg7* mutant, the *cgl71* mutant was unable to grow photoautotrophically, but it did grow photoheterotrophically (mixotrophically) under LO conditions. The LO-grown *cgl71* mutant had lower photosynthetic efficiency than WT cells and had a marked reduction in PSI abundance, with much less of a decline in maximum O_2 evolution per cell. In vivo $P700^+$ rereduction was significantly faster in the LO-grown mutant than in WT cells, indicating more rapid electron flow into PSI in the mutant than in WT cells. Indeed, Fig. S4 shows that the rate of whole-chain electron flow through PSI is faster in the mutant cells than in WT cells; this finding explains why a large reduction in PSI content does not have a correspondingly large impact on whole-chain oxygen evolution.

Previously, Chlamydomonas strains with point mutations in PSI assembly factors (e.g., Ycf3) were shown to grow better under anoxic than oxic conditions (16). The authors of that work reasoned that anoxic conditions reduced the production of reactive oxygen species (ROS) and photodamage. Although this reasoning may be valid, in part, the growth defects of *cgl71* mutants under photoautotrophic and high-light/mixotrophic conditions are also caused by impaired PSI assembly, a process markedly disrupted under more positive stromal redox conditions, even in the dark. The link between the stromal redox state and the level of PSI is clearly demonstrated under DH conditions (in acetate-containing medium), which allow the accumulation of nearly WT levels (∼70% under the conditions used) of PSI. Under air levels of O_2 the mutant cultures lose nearly all PSI in the dark, and the turnover of the polypeptides in the assembled complex also is more rapid in the mutant cells than in WT cells under DO conditions (Fig. S6).

The difference in PSI accumulation in LO and DO conditions probably reflects the difference in stromal redox conditions. Previous studies have shown that the cysteines on the γ-subunit of ATP synthase are oxidized more in the dark than in the light in both vascular plants and Chlamydomonas; this finding could reflect a more general oxidation of thiols associated with chloroplast proteins in the dark (31, 32). Therefore, it is possible that the cysteines associated with other chloroplast components, such as PsaC, also may be more oxidized in the dark, disrupting or destabilizing the assembly of PSI subunits (e.g., PsaC) into PSI in the mutant. As shown by our results, the level of O_2 in the culture severely affects PSI accumulation in the *cgl71* mutant. The O_2 content of the atmosphere increased over evolutionary time, and all organisms on Earth had to adapt to oxic conditions to survive. Therefore, the impact of changing O_2 levels in the atmosphere had to be integrated into cellular regulatory processes and into the assembly and stability of key metabolic complexes. The redox state of the stroma also would affect the activity of thioredoxin-dependent chloroplast enzymes (33). Hence, redox conditions have developed as biological signals that control the cell's energetics (e.g., prevent ATP hydrolysis by the ATP synthase in the dark). Redox conditions also have been shown to have a marked impact on the assembly of viral particles (34), and specific proteins have evolved to protect the biogenesis of the NiFe hydrogenase from disruption by a high O_2 partial pressure (35).

Based on our results, we suggest that proteins have evolved that protect photosynthetic assembly processes from redox/oxidative disruption. CGL71 appears to be most critical for PSI biogenesis/stability under DO conditions and also under high-light oxic conditions, although we could not establish a direct interaction between CGL71 and various PSI subunits (Fig. S7). Under DO conditions, the stroma would tend to be more oxidizing because of the lack of a stromal reductant; the reductant would not be generated by photosynthesis and would be consumed by respiratory processes (mitochondrial electron transport would consume the reductant and generate ATP). Under oxic conditions, photosynthetic electron carriers would become more reduced at lower light levels in the mutant than in WT cells, making the mutant much more prone to photodamage resulting from the increased generation of photosynthetically derived ROS (36). The oxidation–reduction kinetics of PSI centers that assembled in *cgl71* under LO (or DH) conditions exhibited functional characteristics similar to those of WT PSI centers (Fig. 3) and maintained levels of both active cyt b_6f (Fig. S3) and PC (Fig. 2*B*). Furthermore, the charge recombination kinetics of PSI in thylakoid membranes prepared from *cgl71* cells are similar to those of WT cells (Fig. S5). Finally, we observed no functional defect in PSI in the mutant based on our in vitro PSI electron transport assay performed with membranes from lysed cells using MV as an electron acceptor (Fig. S4). Together, these results indicate that PSI that accumulates in *cgl71* cells under LO conditions seems to have normal catalytic function, although, as shown in Fig. S6, the assembled complex may be less stable in the mutant than in WT cells.

The most likely redox-sensitive step in PSI biogenesis is the assembly of the $F_X/F_A/F_B$ Fe-S centers, which previously were found to be highly sensitive to O_2 when exposed to the atmosphere by the removal of the C terminus of PsaC that forms a pocket for tight binding of PSI core subunits (PsaA and PsaB) (37). In addition, the cysteines that bind these Fe-S centers need to be reduced during cofactor insertion. Therefore, it is reasonable to hypothesize that CGL71 is not simply an assembly factor, because the mutant cells assemble active PSI (at high levels) under hypoxic conditions with rates of activity comparable to those of WT cells, but rather that it is critical for protecting the assembling complex from O_2/redox disruption and for the construction of a complex that remains stable in the presence of O_2. This requirement may reflect a direct role in shielding the Fe-S clusters from O_2 exposure or affording protection by facilitating efficient, rapid folding that stabilizes assembled PsaC, PSAD, and PSAE, the proteins that comprise the stromal ridge of the PSI complex and form the ferredoxin-binding pocket.

The above hypothesis also helps explain the difference in phenotypes of the *Synechocystis ycf37* and the *Arabidopsis pyg7* mutants. In cyanobacteria, respiration is performed on the same membranes as photosynthesis. Furthermore, the rate of PSI-driven CEF is much faster in cyanobacteria than in photosynthetic eukaryotes (38). Elevated CEF through the NDH1 pathway and respiratory processes in the cytosol, such as the citric acid cycle and O_2 consumption by cytochrome *c* oxidase, would create a less oxic, more reducing

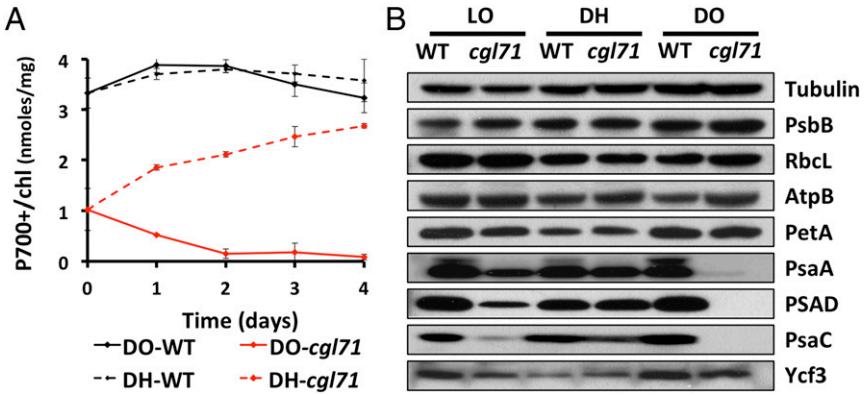

Fig. 4. Changes in PSI during hypoxic growth. Strains were grown under LO conditions for 5 d before being moved to DO or DH conditions for 4 d beginning at day 0. (*A*) Level of oxidizable P700 relative to chl for WT and *cgl71* cells maintained in DO and DH conditions. Points are average values from three saturating flashes. All traces were corrected for potentially interfering absorbance at 740 nm. The results shown represent the average of three biological replicates. (*B*) Immunological detection of specific thylakoid proteins from WT and *cgl71* cells. Proteins extracted from cells containing 1 μg of chl were resolved by SDS/PAGE (15% polyacrylamide gel) and were detected immunologically using monospecific antibodies raised to the polypeptides indicated at the right of the figure. Growth conditions are given at the top of the immunoblot. All protein designations are as in Fig. 2.

environment in the region of assembling photosynthetic complexes in cyanobacteria. Therefore, the loss of Ycf37 in *Synechocystis* would not affect the biogenesis or stability of PSI as severely as the loss of PYG7 does in *Arabidopsis*, where photosynthesis and respiration occur in separate organelles. The photoheterotrophic lifestyle of Chlamydomonas also would serve to lower the stromal redox state as a consequence of acetate oxidation and the movement of reducing equivalents between the mitochondrial and chloroplast compartments. However, in high-light or photoautotrophic conditions, increased O_2 and ROS produced from PET may serve to oxidize components in the stroma and damage membranes and proteins to a point where little PSI can assemble stably in the absence of CGL71 (similar to oxidizing conditions in the stroma under DO conditions).

Cyanobacteria evolved to perform oxygenic photosynthesis ∼3 billion years ago, at a time when the Earth's atmosphere was anoxic (39). Although many of the electron carriers of the photosynthetic apparatus may have been sensitive to O_2, there was little degradation of the machinery because of the lack of O_2 in the atmosphere. As the planet gradually became oxygenated as a consequence of H_2O splitting by photosynthesis, the cytosol must have become more oxic, and PET also would have resulted in the generation of ROS. These environmental pressures may have elicited the evolution of biosynthetic processes that protected O_2-labile components of the photosynthetic apparatus. This study suggests that CGL71 is one of the factors critical for the assembly of PSI under oxic conditions. The concept of protecting the assembly process from oxidative disruption is not exclusive to PSI but is an important consideration when examining the assembly of other multiprotein complexes containing cofactors sensitive to the redox environment.

Materials and Methods

Mutant Generation. The Chlamydomonas *cgl71* mutant was generated by insertion of the *ble* marker gene into the genome of the 4A$^+$ (CC4051) WT strain of Chlamydomonas (40). A complemented strain of the *cgl71* mutant, *cgl71*(CGL71), was generated by transformation of *cgl71* with a WT copy of *CGL71* in the pSL18 plasmid, which carries the *AphVIII* marker gene for paromomycin resistance (41); both marker and rescue genes were expressed from the PSAD promoter (42).

Culture Conditions. The *cgl71* mutant was backcrossed to WT 4A$^+$ at least three times before analysis. Chlamydomonas WT, *cgl71*, and *cgl71*(CGL71) strains were grown in TAP or high-salt HS liquid and solid (1.0% agar) medium. Cultures of 100 mL were shaken in 250-mL Erlenmeyer flasks at 150 rpm under continuous white light of 30 μmol photons·m^{-2}·s^{-1} for LO experiments or were covered with aluminum foil for DO and DH experiments. WT and mutant cells also were grown at other light conditions, as noted in the figures. For experiments performed under DH conditions (Fig. 4*A*), each liquid culture of 400 mL was grown in a 1-L bottle and stirred with a magnetic stir bar at 600 rpm while the medium was continuously purged with 90% N_2:10% air (final 2% O_2) at a flow rate of 400 mL per min.

SDS/PAGE and Immunoblot Analysis. For immunoblot analysis, Chlamydomonas cells were collected by centrifugation (3,500 × *g*, 5 min) after growth under various conditions (described in the main text), resuspended in protein extraction buffer (100 mM Na_2CO_3, 100 mM DTT, and the protease inhibitors 1 mM phenylmethylsulfonyl fluoride, 1 mM ε-amino-n-caproic acid, and 1 mM benzamidine HCl), flash-frozen, and stored at −80 °C. Before electrophoresis, samples were thawed at room temperature, treated immediately with loading buffer containing SDS and sucrose [2% (wt/vol) and 12% (wt/vol) final concentrations, respectively], and then were boiled for 1 min. Cellular debris was removed by centrifugation at 21,000 × *g* for 2 min, and solubilized polypeptides were resolved on a 12% or 4–15% (wt/vol) gradient polyacrylamide gel (Bio-Rad) by SDS/PAGE (30 min, 125-V constant voltage) using the Laemmli buffer system (43). Resolved proteins were transferred from the gel to PVDF membranes which were blocked with a 5% (wt/vol) suspension of powdered milk in Tris-buffered saline with 0.1% Tween-20 before a 1-h incubation in the presence of primary antibodies (23). All primary antibodies were from Agrisera except for α-tubulin, which was from Sigma (T5168), and were used at the dilutions recommended by the manufacturer. HRP-conjugated anti-rabbit IgG (Promega) or IRDye-800CW anti-rabbit IgG (LI-COR), both at a 1:10,000 dilution, were used as the secondary antibodies, and peroxidase activity was detected by chemiluminescence (Advansta).

Chl Measurements. Chl concentrations were determined following extraction of pigments in 1 mL methanol (44) according to the equation: Total chl (μg/mL) = $22.12*A_{652} + 2.71*A_{665}$. The ratio of chl *a* to chl *b* in the sample was determined using the equations of Porra, et al. (44).

PSI/PSII Stoichiometry. Samples were collected during exponential growth, pelleted by centrifugation, and resuspended in Hepes-KOH, (pH 7.2) and 10% Ficoll to a chl concentration of 30 μg/mL. After a 20-min dark-adaptation period, absorbance changes at 520 nm were monitored using a JTS10 spectrophotometer following a saturation pulse by a xenon flash (General Radio Stroboslave) on the high-intensity setting (45). The amplitude of the fast "phase a" in the absence and presence of 20 μM DCMU and 1 mM HA was used to calculate the ratio of PSI/PSII according to Joliot and Delosme (45).

Quantification of Cytochrome *f* Activity. The quantity of cytochrome *f* was determined as described previously (23). The differences between the optical absorption change at 554 nm and the baseline drawn from optical absorption changes at 546 and 573 nm were measured using a JTS-10 spectrophotometer (Bio-Logic) (45). The molar extinction coefficient used to calculate cytochrome *f* quantity was 18,000 M/cm (46).

In Vivo PSII Activity. Chl fluorescence was analyzed using a Walz Dual-PAM-100 fluorometer on the "light curve" setting. Various activities were assayed during a stepped illumination regime; samples (in triplicate) were illuminated for 30 s at each step followed by a saturating light pulse. The yield of PSII at different light intensities was derived from the equation $\Phi PSII = (F_{m'} - F_s)/F_{m'}$ (28, 47).

In Vivo PSI Activity. The activity of photo-oxidizable P700 was measured using a JTS-10 spectrophotometer (Bio-Logic) (45). Before the measurements, cells were incubated with 25 μM DCMU and 1 mM HA to block electron flow out of PSII. To assess PSI redox activity, optical changes at 705 nm were monitored during 5 s of illumination at 156 μmol photons·m^{-2}·s^{-1}, followed by a saturating pulse of 2,265 μmol photons·m^{-2}·s^{-1} and then maintenance of cells in the dark (23). The quantity of $P700^+$ was determined by optical changes at 705 nm subtracted by the kinetic at 740 nm. Upon administration of a saturating pulse, the extinction coefficient used for quantification was 50,000 M/cm (48).

Cloning for Mating-Based Split-Ubiquitin Assay. *CGL71*, *PsaC*, *PSAD*, and *PSAE* genes were amplified from cDNAs using primers listed in Table S1.

ACKNOWLEDGMENTS. We thank John Golbeck for helpful discussions. M.H. was supported by National Science Foundation (NSF) Grant MCB 0951094 (to A.R.G.). R.G.K. and T.M.W. were supported by Stanford Graduate Fellowships, the Biology Department at Stanford University, and the Department of Plant Biology of the Carnegie Institution for Science. W.Y. was supported by US Department of Energy Grant DE-FG02-12ER16338 (to A.R.G.). K.A.W. was supported by NSF Grant Plug and Play II, 657CO. S.K.H. was supported by the College of Agriculture and Natural Resources and the Agricultural Experiment Station at the University of Wyoming.

1. Golbeck JH (1992) Structure and function of photosystem I. *Annu Rev Plant Physiol Plant Mol Biol* 43:293–324.
2. Chitnis PR (2001) PHOTOSYSTEM I: Function and physiology. *Annu Rev Plant Physiol Plant Mol Biol* 52:593–626.
3. Shikanai T (2007) Cyclic electron transport around photosystem I: Genetic approaches. *Annu Rev Plant Biol* 58:199–217.
4. Busch A, Hippler M (2011) The structure and function of eukaryotic photosystem I. *Biochim Biophys Acta* 1807(8):864–877.
5. Kargul J, Janna Olmos JD, Krupnik T (2012) Structure and function of photosystem I and its application in biomimetic solar-to-fuel systems. *J Plant Physiol* 169(16):1639–1653.
6. Amunts A, Nelson N (2008) Functional organization of a plant Photosystem I: Evolution of a highly efficient photochemical machine. *Plant Physiol Biochem* 46(3):228–237.
7. Schöttler MA, Albus CA, Bock R (2011) Photosystem I: Its biogenesis and function in higher plants. *J Plant Physiol* 168(12):1452–1461.
8. Schöttler MA, Tóth SZ (2014) Photosynthetic complex stoichiometry dynamics in higher plants: Environmental acclimation and photosynthetic flux control. *Front Plant Sci* 5:188.
9. Ozawa S, Onishi T, Takahashi Y (2010) Identification and characterization of an assembly intermediate subcomplex of photosystem I in the green alga *Chlamydomonas reinhardtii*. *J Biol Chem* 285(26):20072–20079.
10. Albus CA, et al. (2010) Y3IP1, a nucleus-encoded thylakoid protein, cooperates with the plastid-encoded Ycf3 protein in photosystem I assembly of tobacco and Arabidopsis. *Plant Cell* 22(8):2838–2855.
11. Krech K, et al. (2012) The plastid genome-encoded Ycf4 protein functions as a nonessential assembly factor for photosystem I in higher plants. *Plant Physiol* 159(2):579–591.
12. Spreitzer RJ, Mets L (1981) Photosynthesis-deficient mutants of *Chlamydomonas reinhardii* with associated light-sensitive phenotypes. *Plant Physiol* 67(3):565–569.
13. Hippler M, Biehler K, Krieger-Liszkay A, van Dillewjin J, Rochaix JD (2000) Limitation in electron transfer in photosystem I donor side mutants of *Chlamydomonas reinhardtii*. Lethal photo-oxidative damage in high light is overcome in a suppressor strain deficient in the assembly of the light harvesting complex. *J Biol Chem* 275(8):5852–5859.
14. Barneche F, Winter V, Crèvecoeur M, Rochaix JD (2006) ATAB2 is a novel factor in the signalling pathway of light-controlled synthesis of photosystem proteins. *EMBO J* 25(24):5907–5918.
15. Roose JL, Frankel LK, Bricker TM (2014) The PsbP domain protein 1 functions in the assembly of lumenal domains in photosystem I. *J Biol Chem* 289(34):23776–23785.
16. Naver H, Boudreau E, Rochaix JD (2001) Functional studies of Ycf3: Its role in assembly of photosystem I and interactions with some of its subunits. *Plant Cell* 13(12):2731–2745.
17. Göhre V, Ossenbühl F, Crèvecoeur M, Eichacker LA, Rochaix JD (2006) One of two alb3 proteins is essential for the assembly of the photosystems and for cell survival in Chlamydomonas. *Plant Cell* 18(6):1454–1466.
18. Ossenbühl F, et al. (2004) Efficient assembly of photosystem II in *Chlamydomonas reinhardtii* requires Alb3.1p, a homolog of Arabidopsis ALBINO3. *Plant Cell* 16(7):1790–1800.
19. Pasch JC, Nickelsen J, Schünemann D (2005) The yeast split-ubiquitin system to study chloroplast membrane protein interactions. *Appl Microbiol Biotechnol* 69(4):440–447.
20. Merchant SS, et al. (2007) The Chlamydomonas genome reveals the evolution of key animal and plant functions. *Science* 318(5848):245–250.
21. Karpowicz SJ, Prochnik SE, Grossman AR, Merchant SS (2011) The GreenCut2 resource, a phylogenomically derived inventory of proteins specific to the plant lineage. *J Biol Chem* 286(24):21427–21439.
22. Heinnickel ML, Grossman AR (2013) The GreenCut: Re-evaluation of physiological role of previously studied proteins and potential novel protein functions. *Photosynth Res* 116(2-3):427–436.
23. Heinnickel ML, et al. (2013) Novel thylakoid membrane GreenCut protein CPLD38 impacts accumulation of the cytochrome b_6f complex and associated regulatory processes. *J Biol Chem* 288(10):7024–7036.
24. Calderon RH, et al. (2013) A conserved rubredoxin is necessary for photosystem II accumulation in diverse oxygenic photoautotrophs. *J Biol Chem* 288(37):26688–26696.
25. Fristedt R, Williams-Carrier R, Merchant SS, Barkan A (2014) A thylakoid membrane protein harboring a DnaJ-type zinc finger domain is required for photosystem I accumulation in plants. *J Biol Chem* 289(44):30657–30667.
26. Wilde A, Lünser K, Ossenbühl F, Nickelsen J, Börner T (2001) Characterization of the cyanobacterial *ycf37*: Mutation decreases the photosystem I content. *Biochem J* 357(Pt 1):211–216.
27. Stöckel J, Bennewitz S, Hein P, Oelmüller R (2006) The evolutionarily conserved tetratrico peptide repeat protein pale yellow green7 is required for photosystem I accumulation in Arabidopsis and copurifies with the complex. *Plant Physiol* 141(3):870–878.
28. Maxwell K, Johnson GN (2000) Chlorophyll fluorescence–a practical guide. *J Exp Bot* 51(345):659–668.
29. Baker NR (2008) Chlorophyll fluorescence: A probe of photosynthesis in vivo. *Annu Rev Plant Biol* 59:89–113.
30. Brettel K (1997) Electron transfer and arrangement of the redox cofactors in photosystem I. *Biochim Biophys Acta* 1318(3):322–373.
31. Kramer DM, Crofts AR (1989) Activation of the chloroplast ATPase measured by the electrochromic change in leaves of intact plants. *Biochim Biophys Acta* 976(1):28–41.
32. Wu G, Ortiz-Flores G, Ortiz-Lopez A, Ort DR (2007) A point mutation in *atpC1* raises the redox potential of the *Arabidopsis* chloroplast ATP synthase γ-subunit regulatory disulfide above the range of thioredoxin modulation. *J Biol Chem* 282(51):36782–36789.
33. Kramer DM, et al. (1990) Regulation of coupling factor in field-grown sunflower: A redox model relating coupling factor activity to the activities of other thioredoxin-dependent chloroplast enzymes. *Photosynth Res* 26(3):213–222.
34. Cobbold C, Windsor M, Parsley J, Baldwin B, Wileman T (2007) Reduced redox potential of the cytosol is important for African swine fever virus capsid assembly and maturation. *J Gen Virol* 88(Pt 1):77–85.
35. Fritsch J, Lenz O, Friedrich B (2011) The maturation factors HoxR and HoxT contribute to oxygen tolerance of membrane-bound [NiFe] hydrogenase in *Ralstonia eutropha* H16. *J Bacteriol* 193(10):2487–2497.
36. Asada K (2006) Production and scavenging of reactive oxygen species in chloroplasts and their functions. *Plant Physiol* 141(2):391–396.
37. Jagannathan B, Golbeck JH (2009) Understanding of the binding interface between PsaC and the PsaA/PsaB heterodimer in photosystem I. *Biochemistry* 48(23):5405–5416.
38. Herbert SK, Fork DC, Malkin S (1990) Photoacoustic measurements *in vivo* of energy storage by cyclic electron flow in algae and higher plants. *Plant Physiol* 94(3):926–934.
39. Holland HD (2006) The oxygenation of the atmosphere and oceans. *Philos Trans R Soc Lond B Biol Sci* 361(1470):903–915.
40. Dent RM, Haglund CM, Chin BL, Kobayashi MC, Niyogi KK (2005) Functional genomics of eukaryotic photosynthesis using insertional mutagenesis of *Chlamydomonas reinhardtii*. *Plant Physiol* 137(2):545–556.
41. Sizova IA, et al. (1996) Stable nuclear transformation of *Chlamydomonas reinhardtii* with a *Streptomyces rimosus* gene as the selective marker. *Gene* 181(1-2):13–18.
42. Fischer N, Rochaix JD (2001) The flanking regions of *PsaD* drive efficient gene expression in the nucleus of the green alga *Chlamydomonas reinhardtii*. *Mol Genet Genomics* 265(5):888–894.
43. Laemmli UK (1970) Cleavage of structural proteins during the assembly of the head of bacteriophage T4. *Nature* 227(5259):680–685.
44. Porra RJ, Thompson WA, Kriedemann PE (1989) Determination of accurate extinction coefficients and simultaneous equations for assaying chlorophylls *a* and *b* extracted with four different solvents: Verification of the concentration of chlorophyll standards by atomic absorption spectroscopy. *Biochim Biophys Acta* 975(3):384–394.
45. Joliot P, Delosme R (1974) Flash-induced 519 nm absorption change in green algae. *Biochim Biophys Acta* 357(2):267–284.
46. Pierre Y, Breyton C, Kramer D, Popot JL (1995) Purification and characterization of the cytochrome b_6f complex from *Chlamydomonas reinhardtii*. *J Biol Chem* 270(49):29342–29349.
47. Genty B, Briantais J-M, Baker NR (1989) The relationship between quantum yield of photosynthetic electron transport and quenching of chlorophyll fluorescence. *Biochim Biophys Acta* 990(1):87–92.
48. Hiyama T, Ke B (1972) Difference spectra and extinction coefficients of P 700. *Biochim Biophys Acta* 267(1):160–171.
49. Chua NH, Bennoun P (1975) Thylakoid membrane polypeptides of *Chlamydomonas reinhardtii*: Wild-type and mutant strains deficient in photosystem II reaction center. *Proc Natl Acad Sci USA* 72(6):2175–2179.
50. Grefen C, Obrdlik P, Harter K (2009) The determination of protein-protein interactions by the mating-based split-ubiquitin system (mbSUS). *Methods Mol Biol* 479:217–233.
51. Yang W, et al. (2015) Critical role of *Chlamydomonas reinhardtii* ferredoxin-5 in maintaining membrane structure and dark metabolism. *Proc Natl Acad Sci USA* 112(48):14978–14983.